Nonlinear Dynamics manuscript No.
(will be inserted by the editor)

Design of Delayed Fractional State Variable Filter for Parameter Estimation of Fractional Nonlinear Models

Walid Allafi · Ivan Zijic · Kotub Uddin · Zhonghua Shen · James Marco · Keith Burnham

Received: date / Accepted: date

Abstract This paper presents a novel direct parameter estimation method for continuous-time fractional nonlinear models. This is achieved by adapting a filter-based approach that uses the delayed fractional state variable filter for estimating the nonlinear model parameters directly from the measured sampled input-output data. A class of fractional nonlinear ordinary differential equation models is considered, where the nonlinear terms are linear with respect to the parameters. The nonlinear model equations are reformulated such that it allows a linear estimator to be used for estimating the model parameters. The required fractional time derivatives of measured input-output data are computed by a proposed delayed fractional state variable filter. The filter comprises of a cascade of all-pass filters and a fractional Butterworth filter, which forms the core part of the proposed parameter estimation method. The presented approaches for designing the fractional Butterworth filter are the so-called, square root base and compartmental fractional Butterworth design. According to the results, the parameters of the fractional-order nonlinear ordinary differential model converge to the true values and the estimator performs efficiently for the output error noise structure.

Keywords Delayed fractional state variable filter · Fractional Butterworth filter · Fractional nonlinear system · Parameter estimation · Delay equalisation · Square root base · Compartmental ·

Walid Allafi
WMG, University of Warwick, Coventry, CV4 7AL, U.K
E-mail: w.allafi@warwick.ac.uk

I. Zajic
School of Mechanical, Aerospace and Automotive Engineering, Faculty of Engineering, Environment and Computing, Coventry University, 10 Coventry Innovation Village, Coventry, CV1 2TL, U.K.
E-mail: aa6665@coventry.ac.uk

Kotub Uddin
OVO Energy, 140-142 Kensington Church Street, London W8 4BN, UK
E-mail: kotub.uddin@ovoenergy.com

Zhonghua Shen (✉)
Business School, Guangdong University of Foreign Studies, Guangzhou, China
E-mail: 201610125@oamail.gdufs.edu.cn

James Marco
WMG, University of Warwick, Coventry, CV4 7AL, U.K
E-mail: James.Marco@warwick.ac.uk

Keith Burnham
Faculty of Science and Engineering, University of Wolverhampton, Wulfruna Street, Wolverhampton, WV1 1LY, U.K.
E-mail: K.Burnham@wlv.ac.uk

1 Introduction

Fractional-order systems are proven, through various publications, to have advantages over their integer-order counterparts. The advantages of fractional-order systems over integer order systems include: i) modelling systems by fractional-order allows higher order systems to be expressed by models with fewer parameters, ii) the very nature of many systems lend themselves to be more precisely modelled using fractional-order differential equations as opposed to integer-order differential equations, and iii) fractional-order models of real systems are generally more adequate than commonly adapted integer order models. As such, fractional calculus is attractive to many research fields and hence has encouraged researchers from various fields to extend a significant number of the classical theories and applications to fractional-order [34,13]. Nonlinear and linear fractional-order systems are thus widely applied

in engineering, [17,23] physics [19,54] and control [20, 39,4].

In the case of modelling, which is the focus of this paper, fractional-order nonlinearity has been employed for modelling valve-regulated lead-acid battery systems, described by the nonlinear fractional-order electric equivalent circuit model (NL-FECM) [9,3]. The NL-FECM contains two branches and each branch contains a constant phase element, connected in parallel with a nonlinear resistor. The constant phase element is an expression of a fractional integral element where the nonlinearity appears in both resistors as a function of current (the input of the NL-FECM). The structure of one function is derived from the Butler-Volmer exponential and the other is formulated using the curve fitting approach. The Warburg element represents the diffusional behaviour of the battery and is also characterised by fractional integrals [9]. Linear and nonlinear fractional-order models have also been used to improve the description of thermal dynamic systems [32, 31,30]. In [32], an Aluminum rod was thermally isolated from the surrounding environment to limit the thermal description to only heat conduction with zero heat loss and small temperature variations. In their work [32], the authors employ a fractional-order linear system which significantly improves the performance over small temperature variations via the introduction of a constant heat conductive coefficient. The nonlinearity is observed due to a non-constant conductive coefficient in the case of large temperature variations as shown in [31]. With the presence of a heat loss term, convective and radiative heat transfer appear on the boundary and the radiative heat transfer introduces more nonlinearity to the thermal model [49]. An integer-order chaotic nonlinear system requires a minimum of third order for chaos to appear, based on the Poincare-Bendixon theorem [46]. This is not the same for fractional-order nonlinear systems. For instance, a chaotic attractor is generated by an order as low as 2.7 of Chua's circuit [18] and a sinusoidally driven Duffing system of order less than 2 can still behave in a chaotic manner [24]. Further examples of fractional-order nonlinear system modelling and analysis can be found in [25,36,33].

From a control aspect, fractional-order controllers are widely used for providing robust control. For instance, the fractional-order proportional integral derivative (PID) controller exhibits better performance over classical PID controllers. In particular, for the electrohydraulic servo, because it leads to an improved response, minimum performance indices values, better disturbance rejection, and better sinusoidal trajectory [15]. Several fractional control applications are presented in [7]. In other applications, for instance, systems identification, fractional calculus appears as a fractional least mean square which provides efficient performance in the presence of active noise (Box-Jenkins) for estimating the parameters of linear and nonlinear systems, presented in [37] and [6], respectively.

Fractional nonlinear systems identification has not received major attention because of the complexity associated, mainly, with parameter estimation of the nonlinear fractional-order systems in the continuous-time domain. The benefits of continuous-time models and direct parameter estimation of continuous-time models (not in the discrete domain) have been highlighted in [16]. Continuous-time models are preferred over their discrete-time counterparts because the dynamics of physical systems are generally better described in continuous-time. Continuous-time models also retain a-priori knowledge with inherent data filtering properties. As for direct parameter estimation, then this does not require uniformly sampled data. In addition, significant performance advantages for direct estimation, over indirect approaches, have been reported for a number of classes of systems, including stiff systems. For further details, interested readers are directed to [16].

There are algorithms that have been developed to estimate the parameters of nonlinear fractional-order models, for instance, the differential evolution method. Differential evolution has been used as an algorithm for optimisation purposes and belongs to a class of generic algorithms considered to be a suitable objective function for identifying the orders and parameters of the commensurate fractional-order chaotic systems [43, 29]. The advantages of employing this approach are summarised as follows: (i) it has the capability of finding the actual global minimum, regardless of parameter initialisation accuracy, and (ii) it has the ability of fast convergence with fewer control parameters. The drawbacks of differential evolution, however, include (i) it is designed for a chaotic system and thus needs to be redesigned to cope with a different class of system (ii) convergence is not guaranteed in the case where noise is present, and (iii) the overall estimation problem becomes a complex optimisation problem which is not simple to cope with in different noise scenarios. A different approach based on the Volterra series was presented in [31] to describe the nonlinear diffusive phenomena in a thermal system. In this approach, the Volterra kernel functions are generated by fractional orthogonal bases. The use of Volterra series is motivated by two principal reasons: (i) the separation of linear and the nonlinear contributions due to the decomposition of a nonlinear model and (ii) the Volterra series can be considered as a generalised linear model. In [31], the nonlinear model parameters and linear coefficients are estimated by nonlinear pro-

gramming. However, this approach also involves optimisation and the nonlinear model description is limited to the Volterra structure.

Fractional nonlinear derivative terms are not realizable (measurable) in a majority of systems, which leads to fractional derivative terms being directly approximated from collected data or an equivalent fractional derivative being sought. In the presence of measurement noise, the latter is ill-posed because the approximation amplifies the effects of noise such that finite difference based methods [53,5] become impractical for many applications. This problem is more pronounced for fractional derivatives than integer-order derivatives. To achieve robustness, the B-Spline functions-based fractional differentiator [27], the digital fractional Savitzky-Golay differentiator [12] and the fractional Jacobi differentiator [26] can be assumed, for example. These fractional differentiators are designed in the time domain and built on a polynomial which is used as the unknown signal approximation. The fractional differentiation of this polynomial is used for estimating the required fractional derivatives. The truncation error produced by the polynomial (i.e., the truncated Taylor series expansion of the unknown signal) is retained as an estimation error in the fractional differentiators. This truncations error can generate large errors near the boundaries of the estimating interval, including the noise free signal [28]. To sum up, the approximation of the fractional derivative terms directly from the data show different drawbacks thus the derivative terms for the parameter estimation are replaced by filtered derivative terms using filter base approaches.

On the other hand, in the fractional linear model identification case, different publications have employed a commutative property between known recommended filters and the fractional-order continuous-time linear systems to produce the filtered signal and their derivatives to replace the original signals and their derivatives. The filtered data is utilized for parameter estimation instead of the original data. Examples of linear filters used for this purpose include the Poisson moment functional [11], state variable filters [14], the refined instrumental variable filter [2,47] and the instrumental variable [21]. Unfortunately, the commutative property of the recommended filters is not valid in the case of the fractional-order continuous-time nonlinear systems.

However, Kohr [22] has shown that the delayed state variable filter and the nonlinear derivative terms do commute. Kohr firstly proposed the delayed state variable filter and demonstrated how it could be utilised to estimate the parameters of the continuous-time integer-order nonlinear system, but with very simple nonlinearity. Then in 1994 Tsang and Billing improved the filter to adapt higher order nonlinear terms [45]. The major advantage of the delayed state variable filter is that the commutative property which may allow the techniques used in the linear filter based approach be applicable in the nonlinear case, such as the extra prefiltering technique is used to adapt with coloured noise in the fractional-order linear systems [2]. Due to advantages associated with the delayed state variable filter and fractional-order system properties, the delayed state variable filter is here extended to the delayed fractional state variable filter (DFSVF).

The DFSVF is a cascade of all-pass filters, for group-delay equalisation, with a fractional Butterworth filter (FBF). In the DFSVF, the delayed signals and their higher derivatives are generated by the FBF and are used for subsequent parameter estimation. Therefore, there is also a need to design the FBF. Several authors have published how to extend the approximated integer Butterworth filter to a FBF. For example, Soltan, Rawan and Soliman [41] has extended a two element integer Butterworth filter to a fractional-order in the case of the commensurate order and for higher commensurate order, see [1], where similar coefficients of classical integer Butterworth filter are used for FBF. This filter has been further extended to have two different non-equal base-orders for non-commensurate order in [42]. This is achieved by transforming the FBF to frequency-domain, and then the generated nonlinear equation is optimised to obtain the best flat gain with consideration given to the stability. However, these are not straightforward solutions. Rather they depend on knowledge and experience associated with limited, integer, order. Moreover, in the cited examples, a two element equivalent circuit model is used, where it is relatively easy to adapt fractional-order theory, but this approach becomes increasingly more complex as the number of elements increases.

In this paper, a class of fractional-order nonlinear systems is introduced. This class can be described by a single-input single-output fractional nonlinear ordinary differential equation model. One novelty of this paper is the parameter estimation of this class of systems. The DFSVF is proposed to be directly applied for parameter estimation of the fractional-order continuous-time nonlinear systems from collected input-output data. The process of parameter estimation, using DFSVF, is denoted here by a delayed fractional state variable identification approach. The DFSVF is a cascade of all-pass filters, for group-delay equalisation, with a fractional Butterworth filter (FBF). Two different approached are proposed for the FBF design and are here termed as the square root base and compartmental approaches. In this approach, it is assumed that the system can be

described by an input-output fractional-order nonlinear differential equation. A detailed illustration of how the proposed DFSVF is designed and how this links to the proposed FBF and all-pass filter is provided in this article.

2 Problem statement

A general single-input single-output fractional nonlinear system is described by a fractional nonlinear ordinary differential equation as:

$$A(\mathcal{D}^{\alpha})x(t) + \mathcal{N}(\mathcal{D}^{\kappa}, x(t), u(t)) = B(\mathcal{D}^{\beta})u(t) \tag{1}$$

where $u(t)$ and $x(t)$ denote input and noise-free output signals, respectively. The fractional derivative operator is defined as $\mathcal{D}^{\mu}f(t) = \frac{d^{\mu}f(t)}{dt^{\mu}}$ and $\mu \in \mathbb{R}^{+}$ and $\alpha, \beta, \kappa \in \mathbb{R}^{+}$. $\mathcal{N}$ is a known nonlinear mapping function of $u(t)$, $x(t)$ and the fractional derivative terms, which is defined as fractional polynomial nonlinear function for ease of demonstration in this article. $A(\mathcal{D}^{\alpha})$ and $B(\mathcal{D}^{\beta})$ are output and input fractional linear polynomials in $\mathcal{D}$ defined as:

$$\begin{aligned} A(\mathcal{D}^{\alpha}) &= a_0\mathcal{D}^{\alpha_n} + a_1\mathcal{D}^{\alpha_{n-1}} + \ldots + a_{n-1}\mathcal{D}^{\alpha_1} + a_n \\ B(\mathcal{D}^{\beta}) &= b_0\mathcal{D}^{\beta_m} + b_1\mathcal{D}^{\beta_{m-1}} + \ldots + b_{m-1}\mathcal{D}^{\beta_1} + b_m \end{aligned} \tag{2}$$

where the coefficients $\{a_i, b_j\} \in \mathbb{R}$, $(i = 0, 1, \cdots, n)$, $(j = 0, 1, \cdots, m)$ and the derivative term orders are real and $\alpha_n > \alpha_{n-1} \geq \cdots \geq \alpha_1 > 0$, $\beta_m > \beta_{m-1} \geq \cdots \geq \beta_1 > 0, \alpha_n > \beta_m$. It is assumed $\alpha_0 = \beta_0 = 0$. The model parameter a_n is normalised to be unity, i.e. $a_n = 1$. The fractional polynomial nonlinear function is linear in parameters and does not have a particular description. It is mainly a combination of the nonlinear terms which can have a general form as:

$$\mathcal{N}(\mathcal{D}^{\kappa}, x(t), u(t)) = \sum_{i=0}^{p} v_i N_i(\mathcal{D}^{\kappa_{p-i}}, x(t), u(t)) \tag{3}$$

where $v_i \in \mathbb{R}$, $(i = 0, 1, \cdots, p)$ are estimated model parameters, i.e scalar weighting coefficients, which signify the relative importance of the individual nonlinear functions N_i. The orders of derivative terms of the fractional polynomial nonlinear function are defined as $\kappa_i \leq \kappa_{i+1} \leq \cdots \leq \kappa_p$ and $\kappa_p < \alpha_n$. A uniformly sampled noise-free input-output signals are denoted by $x(t_k)$ and $u(t_k)$, respectively, where the discrete time index is defined as $t_k = kT$ for $k = 1, 2, ...N$ with N being the total number of recorded samples and T is the sampling time interval. The sampled noisy output, denoted $y(t_k)$, is assumed to be corrupted by an addictive discrete white measurement noise $e(t_k)$ and is given by:

$$y(t_k) = x(t_k) + e(t_k) \tag{4}$$

3 Parameter estimation

It is proposed to estimate the model parameters of (1) using the instrumental variable least squares method, see for example [52], while other estimation methods can be clearly utilized. The use of instrumental variables mitigate the impact of additive measurement noise $e(t_k)$ on parameter estimates. Without loss of generality, for ease of derivation and notation, the noise free output $x(t_k)$ will be used instead of $y(t_k)$ for the algorithm derivation. The fractional time derivatives of sampled input-output signals are required by the least squares method and are obtained by the proposed DFSVF, denoted by $\Gamma(\mathcal{D}^{\eta})$. Exploiting the commutative property of the proposed filter the model (1) becomes:

$$\begin{aligned} A(\mathcal{D}^{\alpha})\Gamma(\mathcal{D}^{\eta})x(t) + \mathcal{N}\left(\mathcal{D}^{\kappa}, \Gamma(\mathcal{D}^{\eta})x(t), \Gamma(\mathcal{D}^{\eta})u(t)\right) \\ = B(\mathcal{D}^{\beta})\Gamma(\mathcal{D}^{\eta})u(t) \end{aligned} \tag{5}$$

where the filter acts on all input-output signals. Introducing the filtered input-output variables:

$$\begin{aligned} x_{\Gamma}(t) &= \Gamma(\mathcal{D}^{\eta})x(t) \\ u_{\Gamma}(t) &= \Gamma(\mathcal{D}^{\eta})u(t) \end{aligned} \tag{6}$$

the fractional nonlinear system (5) takes the following filtered form:

$$A(\mathcal{D}^{\alpha})x_{\Gamma}(t) + \mathcal{N}\left(\mathcal{D}^{\kappa}, x_{\Gamma}(t), u_{\Gamma}(t)\right) = B(\mathcal{D}^{\beta})u_{\Gamma}(t) \tag{7}$$

The fractional polynomial nonlinear function is described as a linear combination of nonlinear terms in (3), which allows the fractional nonlinear system (7) to be expressed in the following filtered form:

$$\begin{aligned} a_0\mathcal{D}^{\alpha_n}x_{\Gamma}(t) + a_1\mathcal{D}^{\alpha_{n-1}}x_{\Gamma}(t) + \ldots + a_n x_{\Gamma}(t) + \\ \sum_{i=0}^{p} v_i N_i(\mathcal{D}^{\kappa_{p-i}}, x_{\Gamma}(t), u_{\Gamma}(t)) = \\ b_0\mathcal{D}^{\beta_m}u_{\Gamma}(t) + b_1\mathcal{D}^{\beta_{m-1}}u_{\Gamma}(t) + \ldots + b_m u_{\Gamma}(t) \end{aligned} \tag{8}$$

Consequently, (8) can be reformulated into the linear regression form, used by the linear least squares algorithm, as follows:

$$x_{\Gamma}(t) = \varphi_{\Gamma}^{T}(t)\theta \tag{9}$$

where $\varphi_{\Gamma}^{T}(t)$ and θ denote the filtered regression and parameter vectors, respectively. These are described according to (8) as:

$$\begin{aligned} \varphi_{\Gamma}^{T}(t) = [-\mathcal{D}^{\alpha_n}x_{\Gamma}(t), \ldots, -\mathcal{D}^{\alpha_1}x_{\Gamma}(t), \\ -N_0(\mathcal{D}^{\kappa_p}, x_{\Gamma}(t), u_{\Gamma}(t)), \ldots, -N_p(\mathcal{D}^{\kappa_0}, x_{\Gamma}(t), u_{\Gamma}(t)), \\ \mathcal{D}^{\beta_m}u_{\Gamma}(t), \ldots, u_{\Gamma}(t)] \end{aligned} \tag{10}$$

$$\theta = [a_0, \ldots, a_{n-1}, v_0, \ldots, v_p, b_0, \ldots, b_m] \tag{11}$$

Although the model is originally nonlinear (1), the parameter estimation problem becomes similar to the linear parameter estimation problem by applying the classical state variable filter due to the commutative property between the DFSVF and the nonlinear model (1). This allows extending the off-line estimation to on-line applications. Furthermore, the estimation procedure can be improved to deal with coloured noise processes in a similar manner to the linear case, for instance, by applying the pre-filtering technique for discrete coloured noise [48,40,2] on the generated filtered data in (9).

4 Delayed fractional state variable design

The ideal transport-delay filter can generate a transport-delay for all fractional-order states for all angular frequencies ω. In other words, it is a filter whose gain frequency response is unity and the phase frequency response is denoted $\angle\left(1/\Gamma(j\omega)\right) = -\tau\omega$, for all ω where τ is a constant which is equal to the value of the transport-delay. As a result, the transport-delay (which is the negative derivative of the phase with respect to frequencies ω) is a constant and $T(j\omega) = \tau$ for all frequencies ω. Fig. 1a illustrates the gain, phase and transport-delay axis of the transport-delay filter against ω, where phase and transport-delay axes are expressed in terms of τ.

Although there is no finite order filter that can generate an ideal transport-delay, it is possible to approximate such a filter by introducing some design constraints. Therefore, it is assumed that the ideal transport-delay filter can be designed within a selected range of frequencies ω less than the cut-off frequency denoted ω_c. This generates a group-delay as illustrated in Fig. 1b, for more details on group-delay; see for example the text [51]. This filter is termed an ideal delayed fractional state variable filter. In this paper, the ideal delayed fractional state variable filter is approximated by DFSVF. There are three essential properties must the filter has to be CDFSVF. These properties are the filter has (i) unity gain, (ii) has as constant group-delay as required and (iii) a stable behavior. The DFSVF design starts from selecting the most appropriate basic analogue filter. The Butterworth filter offers a maximally flat gain but associated with this there is a frequency dependent group-delay. In other words, there is a nonlinear phase shift and, furthermore, the rate of change of the phase generally increases as the filters cut-off frequency is approached [8]. However, this unwanted phase distortion and group-delay variation can be corrected and minimised to retain a maximally flat gain by the use of phase-equalising all-pass filters. All-pass filters can be designed to have a group-delay that is virtually complementary to a low-pass filter, so the two filters connected in cascade produce an almost constant group-delay. Therefore, the IBF and all-pass filter are selected for designing the delayed fractional state variable filter, for more details on filters and their properties; see [51,8].

4.1 Fractional Butterworth Filter

The proposed square root base and compartmental FBF designs are based on the classical integer Butterworth filter, which is introduced in detail in following subsections. The approximated (as opposed to ideal) integer Butterworth transfer function can be derived from the maximally flat squared gain function, firstly proposed in [10], and described by a product of the pole terms in [51] as:

$$H_{BW}(s) = \frac{G_0}{\prod_{k=1}^{N}[s - s_k]/\omega_c} \tag{12}$$

$$s_k = \omega_c \left[\cos\left(\frac{\pi}{2} + \pi\frac{2k-1}{2N}\right) + i\sin\left(\frac{\pi}{2} + \pi\frac{2k-1}{2N}\right)\right] \tag{13}$$

where the subscript BW refers to Butterworth filter, ω_c is the cut-off frequency and $s = s_k$ is the k^{th} root for $k = 1, 2, \cdots, N$. The number of roots, denoted N, is user specific and selection guidance is provided in this article. The term G_0 denotes the DC gain, which is selected to be unity, i.e. $G_0 = 1$.

The group-delay of the integer Butterworth filter is the time needed for each frequency component of the filtered signal to pass through the filter and is defined as:

$$T_{BW}(\omega) = -\sum_{k=1}^{N} \frac{\omega_c \cos\left(\frac{\pi}{2} + \pi\frac{2k-1}{2N}\right)}{\omega_c^2 - 2\omega_c\omega\sin\left(\frac{\pi}{2} + \pi\frac{2k-1}{2N}\right) + \omega^2} \tag{14}$$

Fig. 2 shows group delay for an integer Butterworth filter with $\omega_c = 1$. It can be observed that almost flat group-delay is obtained in the low and high frequency ranges with sharp group-delay rise around the cut-off frequency. The higher the order of the filter the higher the group-delay.

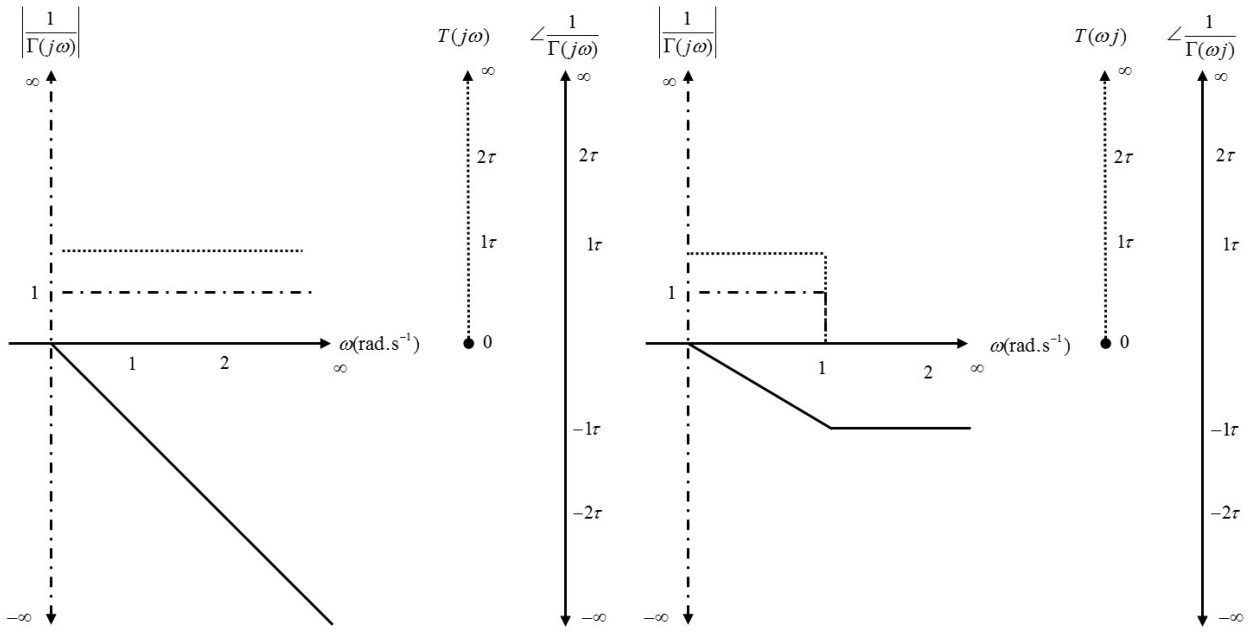

(a) Transport-delay filter. (b) Delayed fractional state variable filter.

Fig. 1: Gain, phase and transport-delay in (a) or group-delay in (b) of $\frac{1}{\Gamma(j\omega)}$, expressed in dashed, solid and dotted lines, respectively where $\omega_c = 1$ $(rad.s^{-1})$.

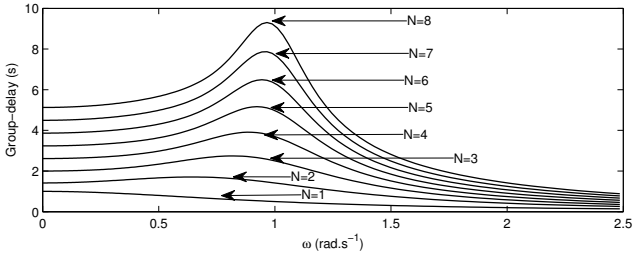

Fig. 2: Group-delay in (s) of the integer Butterworth filter, with order $N = 1 : 8$ and $\omega_c = 1$.

4.1.1 Square root base design (fractional Butterworth filter with $\alpha = 1/2^n$ base-order)

This section demonstrates how the maximally flat gain frequency response of fractional Butterworth filter can be obtained with a restricted base-order $\alpha = 1/2^n$ where $n \in \mathbb{Z}$. There are N root terms in equation (12). When $\alpha = 1$ and N is an even number, the roots in equation (12) are given by $N/2$ complex pairs where $\bar{s}_k$ denotes the conjugate of s_k. Each root term is considered to be a quadratic function, described by the difference of two squares (s and s_k), and expressed in the standard quadratic form and factored form as:

$$\underbrace{s - s_k}_{Standard\ quadratic\ form} = \underbrace{\left(s^{0.5} - \sqrt{s_k}\right)\left(s^{0.5} + \sqrt{s_k}\right)}_{Factored\ quadratic\ form} \tag{15}$$

The factored quadratic form can be obtained by considering the square root of the complex number according to De Moivres theorem:

$$\sqrt[q]{s_k} = \sqrt[q]{|s_k|}\left[\cos\left(\frac{\angle s_k}{q} + \frac{2\pi a}{q}\right) + \sin\left(\frac{\angle s_k}{q} + \frac{2\pi a}{q}\right)\right] \tag{16}$$

where $a = 0, 1$ and N is assumed to be an even number. From equation (15), it can be noted that each root term has two different complex roots $\sqrt{s} = \pm\sqrt{s_k}$. The same techniques are applied to the root term which contains the complex conjugate $\bar{s_k}$ so that the two different conjugate roots $\pm\sqrt{\bar{s_k}}$ are produced. For example, if $N = 2$, the integer Butterworth denominator of equation (12) is described as a product of two root terms as:

$$H_B(s) = \frac{1}{\left(s - \left(\frac{-\sqrt{2}}{2} + j\frac{\sqrt{2}}{2}\right)\right)\left(s - \left(\frac{-\sqrt{2}}{2}j - \frac{\sqrt{2}}{2}\right)\right)}$$

(17)

The factored form of the root term which contains one complex root and the root term which contains the conjugate root can be obtained from equations (15) and (16), and presented as follows:

$$\begin{aligned}\left(s-\left(-\sqrt{2}/2+j\sqrt{2}/2\right)\right)&=\\ \left(s^{0.5}+(0.38+j0.92)\right)\left(s^{0.5}-(0.38+j0.92)\right)&\\ \left(s-\left(-\sqrt{2}/2-j\sqrt{2}/2\right)\right)&=\\ \left(s^{0.5}+(0.38-j0.92)\right)\left(s^{0.5}-(0.38-j0.92)\right)&\end{aligned} \tag{18}$$

The fractional Butterworth transfer function of half-base order, derived from equation (18), is expressed as:

$$\begin{aligned}H_B(s)=\frac{1}{\big[\left(s^{0.5}-0.38+j0.92\right)\left(s^{0.5}-0.38-j0.92\right)}\\ \left(s^{0.5}+0.38+j0.92\right)\left(s^{0.5}+0.38-j0.92\right)\big]\end{aligned}$$

$$\begin{aligned}H_B(s)=\frac{1}{\big[\left(s^{0.25}-0.8315-j0.5556\right)\left(s^{0.25}-0.8315+j0.5556\right)\left(s^{0.25}+0.5556-j0.8315\right)}\\ \left(s^{0.25}+0.5556+j0.8315\right)\left(s^{0.25}+0.8315-j0.5556\right)\left(s^{0.25}+0.8315+j0.5556\right)\\ \left(s^{0.25}-0.5556-j0.8315\right)\left(s^{0.25}-0.5556+j0.8315\right)\big]\end{aligned} \tag{21}$$

The N root terms of the integer Butterworth transfer function produce 2^nN root terms of the fractional Butterworth filter of base-order $\alpha=1/2^n$. For example, the first order Butterworth transfer function generates 2 root terms of a fractional Butterworth filter of base-order $\alpha=0.5$.

(19)

However, in order to avoid returning to the integer-order Butterworth transfer function, the fractional Butterworth transfer function must be described by two subsystems as follows:

$$H_B(s)=\frac{1}{\left(s-0.7654s^{0.5}+1\right)}\frac{1}{\left(s+0.7654s^{0.5}+1\right)} \tag{20}$$

From equation (16), all the fractional derivative terms can be obtained, which can then be used in the identification process.

This can then be factored into eight root terms of base-order $\alpha=0.25$, and it is expressed as (21):

The Butterworth filter of base-order $\alpha=0.25$ in (21) can be described by two first-order subsystems (s^1) or two subsystems whose orders are $(s^{1.5})$ and $(s^{1.5})$ as shown in Fig 4 and, respectively, expressed as (22):

$$\begin{aligned}H_B(s)&=\frac{1}{\left(s+0.0.5518s^{0.75}+0.1522s^{0.5}+0.5518s^{0.25}+1\right)\left(s-0.0.5518s^{0.75}+0.1522s^{0.5}-0.5518s^{0.25}+1\right)}\\ &=\frac{1}{\left(s^{1.25}-1.6629s^{1.25}+1.7654s-1.2728s^{0.75}+1.7645s^{0.5}-1.6629s^{0.25}+1\right)\left(s^{0.5}+1.6629s^{0.25}+1\right)}\end{aligned} \tag{22}$$

The following algorithm can be used to directly generate the roots of the denominator of the fractional Butterworth filter of base-order $\alpha=1/2^n$:

$r=0$
  for $k=1:N$
    $\theta=\pi\left(1/2+(2k-1)/2N\right)$
    for $a=0:m-1$
      $r=r+1$

$$s_k^{\left(1/2^n\right)}=\sqrt[m]{\omega_c}\left[e^{j\left(\theta/m+2\alpha\pi/m\right)}\right] \tag{23}$$

    end
  end

where $m=2^n$, $M=mN$, $a=0,1,\cdots,m-1$ and $k=1,2,\cdots,N$.

The proposed fractional Butterworth filter is derived from the integer Butterworth filter. As a consequence, the frequency response and the group-delay are similar to the frequency response and the group-delay of the integer Butterworth filter. The group-delay of the integer Butterworth filter is shown in Fig 2. Furthermore, the proposed fractional filter is always stable

because it is derived from a stable integer Butterworth filter.

Summary of the design

(i) Design the classical integer Butterworth filter.
(ii) Obtain the factored quadratic form of each root term of the integer Butterworth transfer function by using the complex square roots in (16) for generating the root terms of the fractional Butterworth filter of base-order $\alpha = 1/2$. The fractional Butterworth filter of base-order $\alpha = 1/4$ is then derived from the fractional Butterworth filter of base-order $\alpha = 1/2$. Likewise, the fractional Butterworth filter of base-order $\alpha = 1/2^p$ is then derived from the fractional Butterworth filter of base-order $\alpha = 1/2^{p-1}$ until the targeted base-order is obtained. Furthermore, the roots of the denominator of the fractional Butterworth transfer function of the targeted base-order could be directly derived from the integer Butterworth transfer function by using (23).

4.1.2 Compartmental fractional Butterworth filter design

The proposed compartmental FBF is derived from the integer Butterworth filter which is simulated in Simulink using integer integral block, see [35]. Every integer integral term is compartmentally divided into its equivalent fractional integral terms ($\mathcal{I}f(t) = \int_0^t f(t)dt$), based on the semigroup property of fractional integral of the arbitrary order $\mathcal{I}^{\alpha}\mathcal{I}^{\beta} = \mathcal{I}^{\alpha+\beta}$, stated in [34]. Consequently, the integer integral block in equivalent block diagram form can be represented by a series of fractional integral blocks. This is additional to the property of fractional calculus which takes the fractional derivative term to be the right inverse of the fractional integral term $\mathcal{I}^{\alpha}\mathcal{D}^{\alpha} = \mathbf{I}$, where $\mathbf{I}$ denotes the identity or unity. This property is valid only when considering zero initial conditions, see [34]. Thus, any fractional derivative term can be obtained. This approach can be summarised by the following two steps:

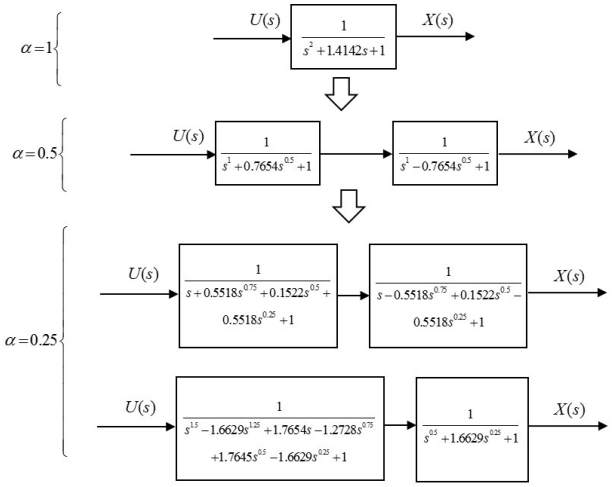

Fig. 3: CFBF of base-order $\alpha = 0.5$ and $\alpha = 0.25$, derived from CIBF where $U(s)$ and $X(s)$ are the input and output of Butterworth filter, respectively.

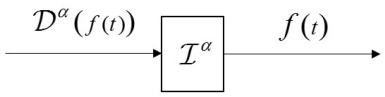

Fig. 4: A block diagram of the fractional integral block.

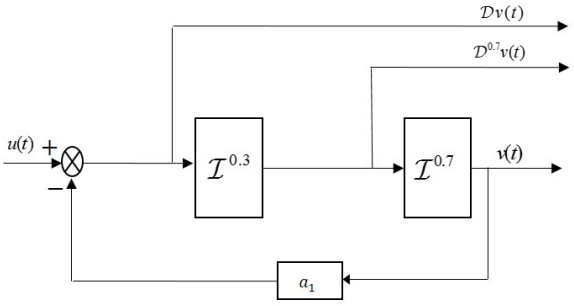

Fig. 5: Compartmental FBF of the first order for approximating the fractional derivative term $\mathcal{D}^{0.7}v(t)$.

For example, if there is a need to approximate an arbitrary α derivative term of the output signal $v(t)$ of the Butterworth filter in Fig. 3, whose order is $N = 1$, the first order integral block can be split into, for example, $\alpha = 0.7$ and $\beta = 0.3$ fractional integral blocks as shown in Fig. 5. Considering the semigroup property it is possible to see that a full integer order integration still takes place, i.e. $\mathcal{I}^{0.7}\mathcal{I}^{0.3} = \mathcal{I}$, hence the functionality of the designed integer Butterworth filter is left intact, but it has been possible to obtain the fractional time derivatives of filtered input-output signals. The fractional integral blocks are available in Simulink via FOMCON Simulink toolbox, for more details see [44].

4.2 Group-delay equalisation: All-pass filter

The designed FBF has been derived based on the classical integer Butterworth filter without changing its non-uniform group-delay. Therefore, it is proposed to adapt the all-pass filter for group-delay equalisation of the FBF, within a selected pass-band, resulting in the overall DFSVF. A second order transfer function of the all-pass filter is expressed as [8]:

$$H_{AP}(s) = \frac{(s-c)^2 + d^2}{(s+c)^2 + d^2} \tag{24}$$

where $c > 0$ for generating a stable filter and the subscript AP denotes all-pass filter. The group-delay of the second order all-pass filter is given by:

$$T_{AP}(\omega) = \frac{4c(\omega^2 + c^2 + d^2)}{(c^2 + d^2 - \omega^2)^2 + 4c^2\omega^2} \tag{25}$$

The overall group-delay of DFSVF is then defined as the sum of the group-delays of all-pass filter and cascaded FBF, where this should equal to a constant, frequency independent, delay, denoted T_0. According to [8], the parameters c and d are then found by solving a following non-linear least squares problem:

$$\epsilon = \int_0^{\omega_{Tmax}} \left[T_0 - T_{BW}(\omega) - T_{AP}(\omega)\right]^2 \tag{26}$$

where $T_{AP}(\omega)$ and $T_{BW}(\omega)$ are the frequency dependent group delays of the all-pass filter and the integer Butterworth filter defined in (25) and (12), respectively. The group delay equalisation is performed only in a predefined low frequency range $\omega = 0$ to $\omega = \omega_{Tmax}$, where at ω_{Tmax} the $T_{BW}(\omega)$ reaches its maximum value.

When increasing the order of integer Butterworth filter the slope of group delay $T_{BW}(\omega)$ (equivalent to the group delay of FBF) becomes more steep and uneven, within the frequency range of interest $\omega = (0, \omega_{Tmax})$, see Fig. 2. Consequently, in order to equalise the group delay $T_{BW}(\omega)$ higher order all-pass filter must be used. So far, the only single second order all-pass filter has been introduced in (24), where higher order all-pass filter can be obtained by cascading several second order all-pass filters into stages. Consequently, as the order of the all-pass filter increases more individual c and d parameters must be found.

In order to assess the performance of the group delay equalisation two following examples are considered. Firstly, a Butterworth filter with cut-off frequency $\omega_c = 1$ $(rad.s^{-1})$ and filter orders ranging from $N = 5$ to $N = 12$ is considered. A two stage all-pass filter is selected, i.e. a cascade connection of two second order $H_{AP}(s)$ filters. The number of stages is denoted M, where $M = 2$ in this example. Table 1 shows the found all-pass filter parameters for stage $M = 1$ and $M = 2$, which are denoted (c_1, d_1) and (c_2, d_2), respectively. The table also shows the found approximated group delay T_0 and ω_{Tmax}. Corresponding Fig. 6 shows the overall obtained group delay of the DFSVF, where the closer the order of the all-pass filter to the order of the Butterworth filter the better equalisation is achieved. This is especially true for orders $N = 5$ and $N = 6$. In other words, selecting the number of the all-pass filter stages mainly depends on the Butterworth order.

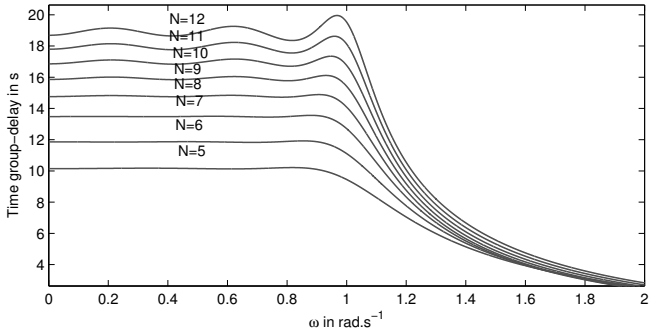

Fig. 6: Group delay of DFSVF with two stage all-pass filter and cut-off frequency $\omega_c = 1$ $(rad.s^{-1})$. The order of Butterworth filter ranges from $N = 5$ to $N = 12$.

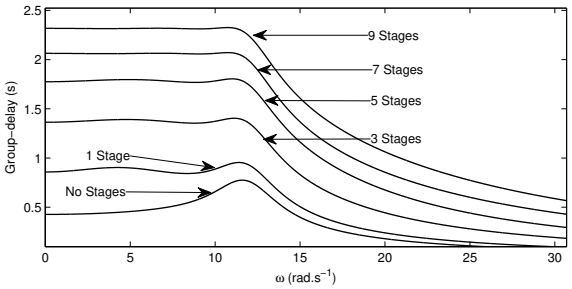

Fig. 7: Group delay of DFSVF with stages of all-pass filter ranging from $M = 1$ to $M = 9$. The order of Butterworth filter is $N = 8$ with cut-off frequency $\omega_c = 12$ $(rad.s^{-1})$. The case when no all-pass filter is used is also shown, i.e. only the group delay of the Butterworth filter is plotted.

Secondly, a Butterworth filter with cut-off frequency $\omega_c = 12$ $(rad.s^{-1})$ and a fixed order $N = 8$ is chosen. All-pass filter stages range from $M = 1$ to $M = 9$ are shown in 7. Table 2 shows the found all-pass filter parameters for all stages as well as the approximated delay T_0. In general, the higher the number of stages the better equalisation is achieved and the higher the value of the approximated group delay T_0 is obtained.

Table 1: Parameters of two stage all-pass filter when equalizing a Butterworth filter with cut-off frequency $\omega_c = 1$ $(rad.s^{-1})$ and orders ranging from $N = 5$ to $N = 12$.

Butterworth filter Orders	c_1	d_1	c_2	d_2	T_0 (s)	ω_{Tmax} $(rad.s^{-1})$
$N = 5$	0.7310	0.5594	1.1570	0.0000	10.1581	0.9236
$N = 6$	0.5766	0.6269	0.8300	0.0000	11.8575	0.9443
$N = 7$	0.4765	0.6723	0.5611	0.2198	13.4829	0.9574
$N = 8$	0.4086	0.6747	0.4617	0.2245	14.7928	0.9663
$N = 9$	0.3662	0.6675	0.4074	0.2219	15.9344	0.9726
$N = 10$	0.3366	0.6559	0.3708	0.2185	16.9856	0.9772
$N = 11$	0.3145	0.6504	0.3439	0.2152	17.9797	0.9807
$N = 12$	0.2972	0.6422	0.3229	0.2121	18.9351	0.9835

Table 2: All-pass filter parameters for stages ranging from $M = 1$ to $M = 9$. Butterworth filter cut-off frequency is $\omega_c = 12$ $(rad.s^{-1})$ and order $N = 8$.

T_0	i	$M = 1$	$M = 2$	$M = 3$	$M = 4$	$M = 5$	$M = 6$	$M = 7$	$M = 8$	$M = 9$
0.8819	c_i	5.6700	–	–	–	–	–	–	–	–
	d_i	4.5222	–	–	–	–	–	–	–	–
1.3769	c_i	8.9502	8.9500	8.9504	–	–	–	–	–	–
	d_i	5.8805	5.8806	5.8806	–	–	–	–	–	–
1.7856	c_i	10.698	10.698	10.698	10.698	10.698	–	–	–	–
	d_i	6.6533	6.6533	6.6534	6.6533	6.6533	–	–	–	–
2.0622	c_i	18.087	13.377	20.439	15.491	17.316	17.140	5.8819	–	–
	d_i	0.8265	2.7210	1.1312	1.4624	0.8546	0.8785	8.6657	–	–
2.3167	c_i	19.450	19.870	19.484	19.557	20.317	19.572	21.230	14.687	5.9750
	d_i	0.4351	0.6444	0.4578	0.4910	0.8413	0.5015	1.1094	0.1490	8.7329

5 DFSVF implementation and estimation process

The implementation and simulation of the delayed state variable filter are essential steps to proper parameter estimation. The system of equation defined in the state space representation or a transfer function can be expressed in an equivalent block diagram as a state variable filter and more information can be found in [36, 2]. The equivalent block diagram allows collecting the derivatives of the signals in clearer and easier manner by implementing it in Simulink. It is then numerically solved at each sample by using one of the Simulink solvers such as the Euler or Runge-Kutta solver.

In previous sections, FBF and all-pass filter are individually treated. However, all these filters can be combined in one filter called delayed fractional state variable filter for generating delayed fractional derivative terms whether they are linear or nonlinear. Thus, the delayed state variable filter is simulated in two steps as illustrated in Fig. 8. The all-pass filters are firstly and individually cascaded and simulated in Simulink.

The output of the cascaded all-pass filters is used as an input to simulate the fractional Butterworth filter in Simulink. From fractional Butterworth filter, all the higher fractional derivative terms of the filtered signals can be obtained. For instance, an arbitrary signal $y(t)$ is passed through the delayed fractional state variable filter. Consequently, the filtered or delayed $y(t)$ is produced and denoted $y_\Gamma(t)$. Furthermore, all the higher fractional derivative terms $\mathcal{D}^{\alpha_i} y_\Gamma(t)(t) = \frac{d^{\alpha_i} y_\Gamma(t)(t)}{dt^{\alpha_i}}$ can be collected from fractional Butterworth.

Fig. 8 demonstrates the input and the outputs of the delayed fractional state variable filter where in later sections the input will be the signals, which are collected for identification. The system simulation and identification process steps are illustrated in Fig. 9.

6 Simulation study

This section addresses the comparison between the proposed approaches and the numerical example for nonlinear system estimations.

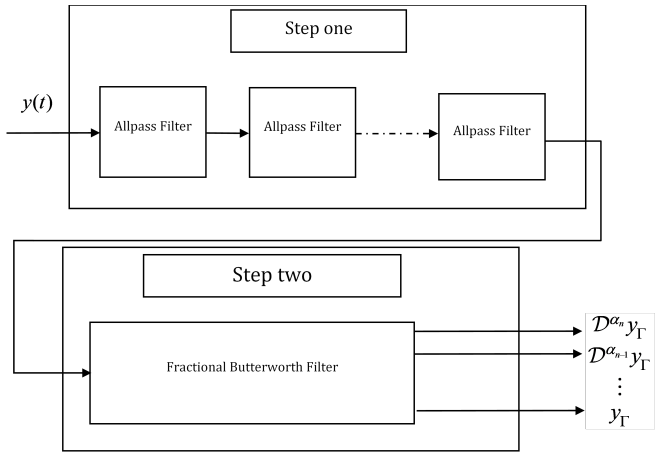

Fig. 8: Block Diagram of the delayed state variable filter simulation.

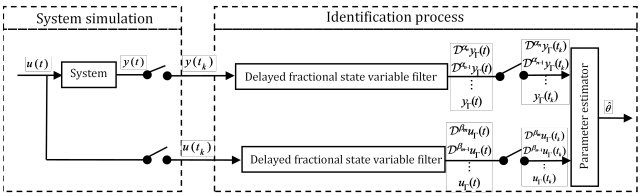

Fig. 9: System simulation and identification process.

6.1 Comparison of the proposed approaches

Two approaches for designing the fractional-order Butterworth filter has been proposed in this paper, namely, the square root base design and compartmental fractional-order Butterworth filter design.

The comparison made in this section is used to support the selection of one approach to be used in approximating the higher fractional-order derivative terms of the output of the Butterworth filter in the numerical example that will foloow. Accordingly, in this section, an illustrative example is used as a benchmark to evaluate the performance of the two proposed approaches. The second order classical Butterworth filter is used as a reference to validate both approaches and is also used to approximate the higher fractional-order derivative terms. For instance, if we take the Butterworth output $v(t)$ and $\mathcal{D}^{0.25}v(t)$ are the collected targets. The square root base fractional Butterworth filter (SRBFBF) is second order and is shown in Fig. 10. It can be observed that this approach has eight fractional-order integral blocks. This requires computational time compared to the compartmental fractional Butterworth filter (CFBF) which only has three fractional-order integral blocks, as illustrated in Fig. 11. The simulation runs for 5 s by using Simulink and MATLAB®. The solver is selected to be Runge-Kutta with 0.001s sampling time. Fractional-order integral blocks are from The FOMCON Simulink block library where approximation order and frequency range are set to fifth order and [0.001; 100] $rad.s^{-1}$, respectively. The input is selected as a sum of the sinusoid signals within the range of the fractional-order integral blocks range as illustrated in Fig. 12. The integral of the absolute error (IAE) between the output and higher fractional-order derivative terms, obtained from the integer-order Butterworth filter, are compared with those obtained by the CFBF and SRBFBF.

The Butterworth filter output, the $\mathcal{D}v(t)$ terms based on the three different designs and the $\mathcal{D}^{0.25}v(t)$ terms of both fractional-order filter designs are shown in Figs. 13, 14, and Table 3. It can readily be seen from Table 3 that the CFBF provides a better approximation to the reference filter, i.e. the classical Butterworth filter, as compared to the SRBFBF in terms of IAE measure. This improved filtering performance of CFBF is further visible in Figs. 13, 14, where the filtered signals are seen to be closer to their reference counterpart. The error that is present is the numerical error associated with each fractional-order integral block. This error scales with the number of fractional-order integral blocks used and consequently more pronounced for the SRBFBF. The results, obtained from 13, and Table 3, favour selection of the compartmental approach over the square root approach. It is noteworthy to highlight that:

(I) The design process of the compartmental approach is considerably simpler than the square root based approach.

(II) The compartmental approach can be applied to obtain any fractional-order, which is not the same with the square root based approach that is limited by base-order $\alpha = {}^1/_{2^n}$.

(III) A higher numerical accuracy is achieved using the compartmental approach relative to the square root based approach for approximation of the same fractional-order derivative term.

(IV) The computational time of the compartmental approach is relatively smaller than the computational time of the square root approach.

(V) The compartmental approach presented better capability in generating any arbitrary fractional-order derivative terms.

This leads to the compartmental approach being the favourable method; adopting this method also increases the adaptability to non-commensurate systems.

The major advantages of the proposed designs and filters over the published approaches are their generality and simplicity. Several authors have published on

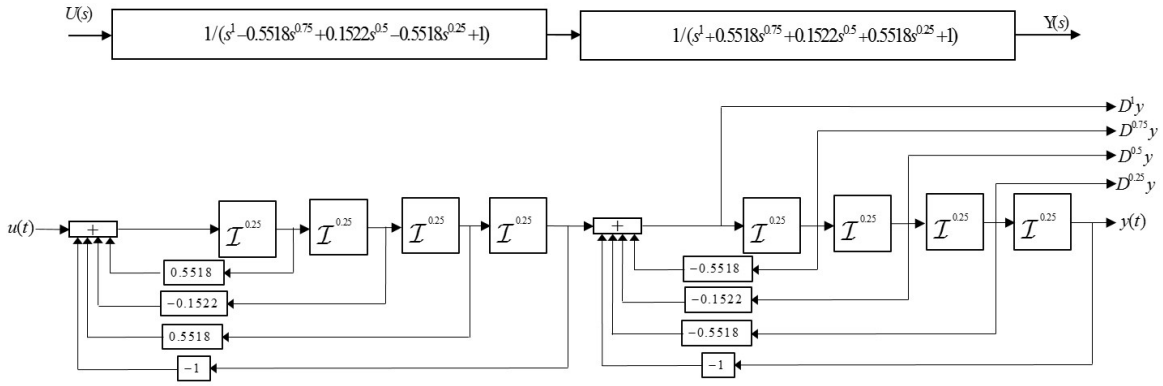

Fig. 10: The upper part shows the transfer function of the two subsystems representing fractional-order-Butterworth filter and the equivalent block diagram by applying square root base for base-order $\alpha = 1/2$ where $\alpha = 1/4$ and $\omega_c = 1$.

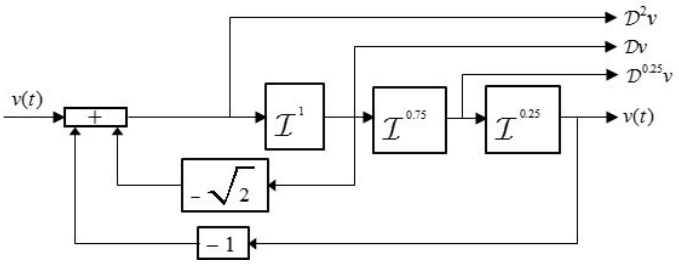

Fig. 11: Second order fractional-order Butterworth filter using compartmental approach where $\omega_c = 1$.

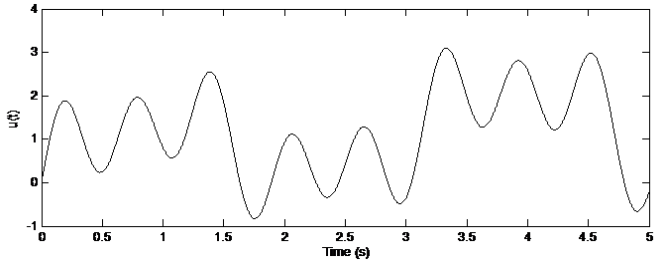

Fig. 12: Input is used for simulation.

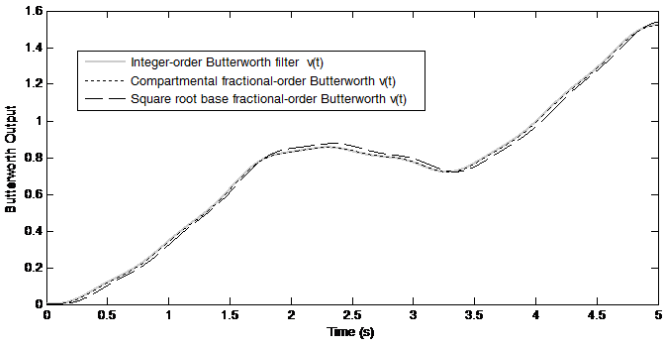

Fig. 13: Bold grey solid-line is the integer-order Butterworth filter output $v(t)$, black doted-line and black dashed-line represent the CFBF output $v(t)$ and the SRBFBF output $v(t)$, respectively.

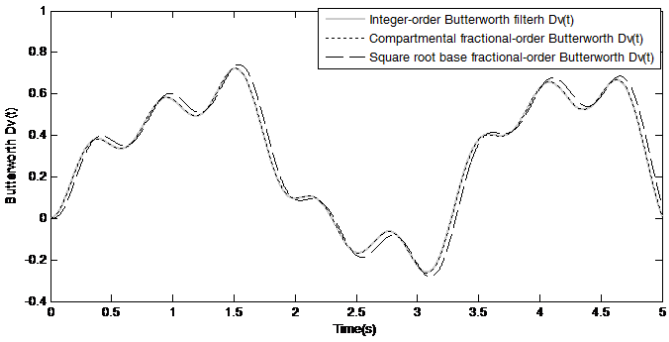

Fig. 14: Bold grey solid-line is the derivative term $\mathcal{D}v(t)$ of the integer-order Butterworth filter and black doted-line and black dashed-line represent the derivative terms $\mathcal{D}v(t)$ of CFBF and SRBFBF, respectively.

how to extend the approximated integer Butterworth filter to an FBF. For example, Soltan, Rawan and Soliman [41] have extended a two element integer Butterworth filter to fractional-order in the case of the commensurate order and higher commensurate orders, see [1]. In their work, similar coefficients of a classical integer Butterworth filter are used for FBF. This filter was been further extended to have two different non-equal base-orders for non-commensurate orders in [42]. This is achieved by first transforming the FBF to the frequency-domain. The generated nonlinear equation is then optimised to obtain the best flat gain, with consideration given to stability. However, these are no straightforward solutions. Rather, they depend on knowledge and experience associated with limited, integer, orders. Moreover, in the cited examples, a two element

Table 3: The calculated IAE performance measure together with corresponding frequency ranges for different integer model orders of approximated fractional models.

	IBF	CFBF	SRBFBF
Computational time	0.4228s	0.9568s	1.0270s
	0	0.0036	0.0180
	0	0.0015	0.0262

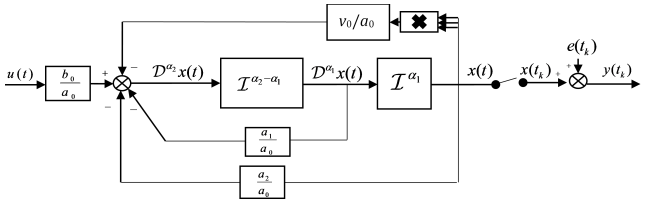

Fig. 15: The equivalent block diagram of (27) with considering noise.

equivalent circuit model is used, where it is relatively easy to adapt fractional-order theory, but this approach becomes increasingly more complex as the number of elements increase.

6.2 Numerical example

The performance of the presented delayed fractional state variable identification approach is demonstrated on a parameter estimation problem of fractional nonlinear Duffing's oscillator [36]. The system model is described by a following ordinary fractional nonlinear differential equation:

$$\mathcal{S}\begin{cases} a_0\mathcal{D}^{\alpha_2}x(t) + a_1\mathcal{D}^{\alpha_1}x(t) + a_2x(t) + v_0x^3(t) = b_0u(t) \\ y(t_k) = x(t_k) + e(t_k) \end{cases} \tag{27}$$

where the measured output is corrupted by additive, white, zero mean noise with Gaussian distribution with variance σ_e^2. The noise variance is selected such that a prescribed signal to noise ratio, denoted SNR, is achieved. The SNR is defined in dB by $10\log(\sigma_x^2/\sigma_e^2)$, where σ_x^2 denotes the variance of noise free system output $x(t)$. The model parameters are chosen to be: $a_0 = 1$, $a_1 = 1$, $v_0 = 0.6$, $b_0 = 1$ and parameter a_2 is normalised to unity. Two fractional order cases are considered, firstly, commensurate with $\alpha_1 = 0.5$ and $\alpha_2 = 1$ and, secondly, non-commensurate fractional order with $\alpha_1 = 0.7$ and $\alpha_2 = 1$.

The system in (27) can be simulated in Simulink by using equivalent block diagram as shown in Fig. 15.

The input signal is selected to be a sum of 10 sinusoids whose bandwidth is $\omega = 1$ $(rad.s^{-1})$. The highest frequency of system, required to be covered is approximately 3-5 times the bandwidth of the input signals. This is because for low pass characteristics and systems having mild nonlinearities, the response of the system output can be well tackled by the first 3-5 Volterra kernels [50].

This simulation has been run over a time period of 50 (s) with a simulation time step of $T_s = 0.001$ (s). The selected Simulink solver is ode4 (Runge-Kutta). The Simulink fractional integral block-set, required to implement FBF, is provided by FOMCON Simulink library with the following setting: The interesting frequency range of the fractional integral term has been selected to be $[0.001, 1000]$ $(rad.s^{-1})$ in order to guarantee the noise in high frequencies is not filtered by the integral approximation. The FOMCON library uses the modified Oustaloup method and the coefficient selection is connected more to the numerical study requirements but not connected with the DFSVF implementation. There are more numerical methods for approximating the fractional integral terms such as Carlson's and Matsuda's methods [38]. The DFSVF has been designed with eighth order FBF, $N = 8$, and cut-off frequency of $\omega_c = 12$ $(rad.s^{-1})$. Nine stages of the second order all-pass filter, $M = 9$, are chosen to achieve approximately constant group-delay. The bandwidth of the Butterworth filter is selected to handle the entire output range of frequencies.

Figs. 16a, 16b and 17 show the performance of the selected commensurate DFSVF applied to system input and output signals, respectively, with $SNR = 20dB$. For example, considering Fig. 16a, the filtered input signal (solid black line) is delayed approximately by 2.3 (s), while only little to no shape distortion is cased by the filtering process, as expected. Furthermore, the noise in the filtered output has been significantly reduced as shown Fig. 16b because the DFSVF performs as a low pass filter. Fig. 17 shows the noise-free fractional signal derivatives $\mathcal{D}^{0.5}x(t)$ (solid black line) and $\mathcal{D}x(t)$ (dashed black line) and their corresponding filtered measured counterparts $\mathcal{D}^{0.5}y(t)$ (solid grey line), and $\mathcal{D}y(t)$ (dashed grey line), respectively. A small shape distortion of the filtered derivative signals is visible in Fig. 17 due to relatively high signal to noise ratio, as expected, indicating a high performance of the designed DFSVF.

Table 4 presents Monte Carlo simulation study results, where 50 runs with random measurement noise realisation for each run are considered. The mean and

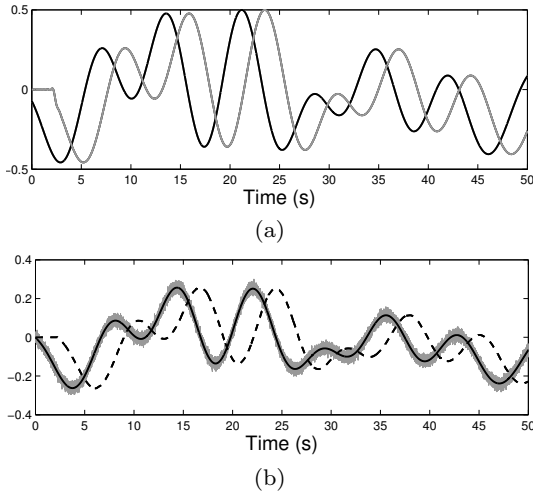

Fig. 16: Subplot (a) shows sampled input signal $u(t)$ (solid grey line) and filtered input $u_{\Gamma}(t)$ (solid black line). Subplot (b) shows noise-free output $x(t)$ (dashed black line), measured noisy output $y(t)$ (solid grey line), and filtered noisy output $y_{\Gamma}(t)$ (dashed black line). Commensurate system order is considered for $SNR = 20dB$.

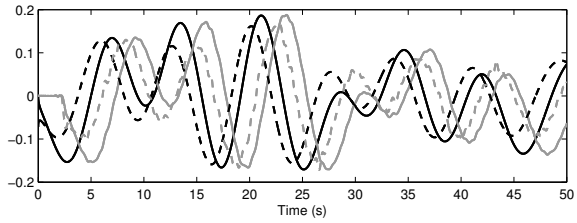

Fig. 17: Noise-free fractional signal derivatives $\mathcal{D}^{0.5}x(t)$ (solid black line) and $\mathcal{D}x(t)$ (dashed black line) with their corresponding filtered measured counterparts $\mathcal{D}^{0.5}y(t)$ (solid grey line) and $\mathcal{D}y(t)$ (dashed grey line).

standard deviations of parameter estimates are presented for comparing the statistical efficiency of the proposed identification approach. Two different noise strengths scenarios are evaluated with low $SNR = 10dB$ and high $SNR = 20dB$. The obtained results indicate a high parameter estimation accuracy for both the commensurate and non-commensurate system orders despite the presence of significant measurement noise.

7 Conclusions

The delayed fractional state variable identification approach for parameter estimation of a class of fractional nonlinear ordinary differential equation models, in the continuous-time domain, has been presented. The core part of this approach comprises of the proposed delayed fractional state variable filter (DFSVF) in a connection with a suitable parameter estimation method. The DFSVF contains a cascade of all-pass filters, for group delay equalisation, and proposed, a novel, fractional Butterworth filter (FBF).

The comparison study illustrates that the compartmental fractional Butterworth filter (CFBF) showed better performance in the delayed fractional state variable identification approach over the square root base fractional Butterworth (SRBFB) of in terms of generality (the proposed CFBF can generate any arbitrary fractional terms while SRBFB is limited with base-order $\alpha = {}^{1}/_{2^n}$), simplicity and computational accuracy and computational time. However, both approaches and FBF offer the following advantages: i) they are simpler in derivation because they are built on the well-known integer Butterworth filter. The extra step is to use well-known properties of the integral and avoiding the use of optimisation algorithms or square roots of complex terms; iii) the performance of the proposed FBF generates and guarantees maximum flat gain because it holds the properties of the integer Butterworth filter; and iv) the proposed compartmental and square root base approaches can be mapped to extend any other linear filter directly from the classical integer linear filter.

The required property of the DFSVF is to have a maximally flat magnitude response and constant group delay in a selected frequency band in order to achieve the required commutative property for subsequent model parameter estimation. It has been revealed that the order of all-pass filter depends on the order of fractional Butterworth filter and the selected cut-off frequency of DFSVF.

The presented delayed fractional state variable identification approach is demonstrated on a parameter estimation problem of fractional nonlinear Duffings oscillator and its performance has been assessed via a Monte-Carlo simulation study. The measured, sampled, input-output data were used to show the practicality of the proposed method. A consistent performance has been achieved for various noise strength scenarios with small standard deviations of parameter estimates.

In addition to the advantages of the aforementioned CFBF and SRBFBF, the properties of a low pass-filter allow the DFSVF to reduce the effect of high frequency noise. The commutative property of DFSVF further allows the nonlinear estimation problem to be expressed as a linear estimation problem by using the classical state variable filter. This increases the possibility of canceling the effect of coloured noise directly from the filtered (delayed) data by, for instance, using pre-filtered techniques and extending the proposed algorithm to an

Table 4: Monte Carlo simulation results for fractional-order continuous-time nonlinear commensurate ($\alpha_1 = 0.5, \alpha_2 = 1$) and non-commensurate ($\alpha_1 = 0.7, \alpha_2 = 1$) system.

System order	SNR	true	$a_0 = 1$	$a_1 = 1$	$v_0 = 0.6$	$b_0 = 1$
Commensurate	10dB	*mean*	1.0012	1.0013	0.6289	1.0010
		std	0.0131	0.0301	0.2271	0.0120
	20dB	*mean*	1.0004	1.0004	0.6091	1.0003
		std	0.0041	0.0095	0.0713	0.0038
Non-commensurate	10dB	*mean*	1.0003	1.0035	0.6191	1.0014
		std	0.0193	0.0279	0.1625	0.0087
	20dB	*mean*	1.0001	1.0011	0.6061	1.0004
		std	0.0061	0.0088	0.0512	0.0027

on-line application. This extends the applicability of the proposed approach to fields of model based systems monitoring, fault detection, adaptive observer design, and adaptive control.

For further work, the proposed approach will be compared with other approaches such as the optimisation based approaches to highlight strengths and weaknesses in light of different noise processes.

Conflicts of interest: All authors declare that they have no conflict of interest.

References

1. Acharya, A., Das, S., Pan, I., Das, S.: Extending the concept of analog butterworth filter for fractional order systems. Signal Processing **94**, 409–420 (2014)
2. Allafi, W., Burnham, K.J.: Identification of fractional-order continuous-time hybrid box-jenkins models using refined instrumental variable continuous-time fractional-order method. In: Advances in Systems Science - Proceedings of the International Conference on Systems Science, pp. 785–794 (2013)
3. Allafi, W., Uddin, K., Zhang, C., Sha, R.M.R.A., Marco, J.: On-line scheme for parameter estimation of nonlinear lithium ion battery equivalent circuit models using the simplified refined instrumental variable method for a modified wiener continuous-time model. Applied Energy **204**, 497 – 508 (2017). DOI http://dx.doi.org/10.1016/j.apenergy.2017.07.030
4. Allafi, W., Zajic, I., Burnham, K.J.: Identification of Fractional Order Models: Application to 1D Solid Diffusion System Model of Lithium Ion Cell, pp. 63–68. Springer International Publishing, Cham (2015)
5. Anderson, S.R., Kadirkamanathan, V.: Modelling and identification of non-linear deterministic systems in the delta-domain. Automatica **43**(11), 1859–1868 (2007)
6. Aslam, M.S., Chaudhary, N.I., Raja, M.A.Z.: A sliding-window approximation-based fractional adaptive strategy for hammerstein nonlinear armax systems. Nonlinear Dynamics **87**(1), 519–533 (2017). DOI 10.1007/s11071-016-3058-9
7. Azar, A., Vaidyanathan, S., Ouannas, A.: Fractional order control and synchronization of chaotic systems, vol. 688. Springer (2017)
8. Blinchikoff, H.J.: Filtering in the Time and Frequency Domains. Electromagnetic Waves. Institution of Engineering and Technology (2001)
9. Buller, S., Thele, M., Karden, E., Doncker, R.W.D.: Impedance-based non-linear dynamic battery modeling for automotive applications. Journal of Power Sources **113**(2), 422 – 430 (2003). DOI https://doi.org/10.1016/S0378-7753(02)00558-X. Proceedings of the International Conference on Lead-Acid Batteries, {LABAT} '02
10. Butterworth, S.: On the theory of filter amplifiers. Wireless Engineer **7**(6), 536–541 (1930)
11. Cahoy, D.O., Uchaikin, V.V., Woyczynski, W.A.: Parameter estimation for fractional poisson processes. Journal of Statistical Planning and Inference **140**(11), 3106 – 3120 (2010). DOI http://dx.doi.org/10.1016/j.jspi.2010.04.016
12. Chen, D., Chen, Y., Xue, D.: Digital fractional order savitzky-golay differentiator. IEEE Transactions on Circuits and Systems II: Express Briefs **58**(11), 758–762 (2011). DOI 10.1109/TCSII.2011.2168022
13. Chen, Y., Wei, Y., Zhou, X., Wang, Y.: Stability for nonlinear fractional order systems: an indirect approach. Nonlinear Dynamics **89**(2), 1011–1018 (2017). DOI 10.1007/s11071-017-3497-y. URL https://doi.org/10.1007/s11071-017-3497-y
14. Cois, O., Oustaloup, A., Poinot, T., Battaglia, J.L.: Fractional state variable filter for system identification by fractional model. In: 2001 European Control Conference (ECC), pp. 2481–2486 (2001)
15. Essa, M., Aboelela, M., Hassan, M.: Application of fractional order controllers on experimental and simulation model of hydraulic servo system. In: Fractional Order Control and Synchronization of Chaotic Systems, pp. 277–324. Springer (2017)
16. Garnier, H., Wang, L., Young, P.C.: Direct Identification of Continuous-time Models from Sampled Data: Issues, Basic Solutions and Relevance, pp. 1–29. Springer London, London (2008)
17. Gutiérrez, R.E., Rosário, J.M., Tenreiro Machado, J.: Fractional order calculus: basic concepts and engineering applications. Mathematical Problems in Engineering **2010** (2010)
18. Hartley, T.T., Lorenzo, C.F., Qammer, H.K.: Chaos in a fractional order chua's system. IEEE Transactions on Circuits and Systems I: Fundamental Theory and Applications **42**(8), 485–490 (1995). DOI 10.1109/81.404062
19. Hilfer, R.: Applications of fractional calculus in physics. World Scientific (2000)

20. Karami-Mollaee, A., Tirandaz, H., Barambones, O.: On dynamic sliding mode control of nonlinear fractional-order systems using sliding observer. Nonlinear Dynamics **92**(3), 1379–1393 (2018). DOI 10.1007/s11071-018-4133-1. URL https://doi.org/10.1007/s11071-018-4133-1
21. Khadhraoui, A., Jelassi, K., Trigeassou, J.C., Melchior, P.: Identification of fractional model by least-squares method and instrumental variable. Journal of Computational and Nonlinear Dynamics **10**(5), 050801–01–10 (2015)
22. Kohr, R.H.: A method for the determination of a differential equation model for simple nonlinear systems. Electronic Computers, IEEE Transactions on **EC-12**(4), 394–400 (1963)
23. Leyden, K., Goodwine, B.: Fractional-order system identification for health monitoring. Nonlinear Dynamics **92**(3), 1317–1334 (2018). DOI 10.1007/s11071-018-4128-y. URL https://doi.org/10.1007/s11071-018-4128-y
24. Li, Z., Chen, D., Zhu, J., Liu, Y.: Nonlinear dynamics of fractional order duffing system. Chaos, Solitons & Fractals **81, Part A**, 111 – 116 (2015). DOI https://doi.org/10.1016/j.chaos.2015.09.012
25. Lin, J., Wang, Z.J.: Parameter identification for fractional-order chaotic systems using a hybrid stochastic fractal search algorithm. Nonlinear Dynamics **90**(2), 1243–1255 (2017). DOI 10.1007/s11071-017-3723-7. URL https://doi.org/10.1007/s11071-017-3723-7
26. Liu, D.Y., Gibaru, O., Perruquetti, W., Laleg-Kirati, T.M.: Fractional order differentiation by integration and error analysis in noisy environment. IEEE Transactions on Automatic Control **60**(11), 2945–2960 (2015). DOI 10.1109/TAC.2015.2417852
27. Liu, D.Y., Laleg-Kirati, T.M., Gibaru, O., Perruquetti, W.: Fractional Order Numerical Differentiation with B-Spline Functions. In: The International Conference on Fractional Signals and Systems 2013. Ghent, Belgium (2013)
28. Liu, D.Y., Zheng, G., Boutat, D., Liu, H.R.: Non-asymptotic fractional order differentiator for a class of fractional order linear systems. Automatica **78**, 61 – 71 (2017). DOI http://dx.doi.org/10.1016/j.automatica.2016.12.017
29. Liu, F., Li, X., Liu, X., Tang, Y.: Parameter identification of fractional-order chaotic system with time delay via multi-selection differential evolution. Systems Science & Control Engineering **5**(1), 42–48 (2017)
30. Maachou, A., Malti, R., Melchior, P., Battaglia, J.L., Hay, B.: Thermal system identification using fractional models for high temperature levels around different operating points. Nonlinear Dynamics **70**(2), 941–950 (2012). DOI 10.1007/s11071-012-0507-y. URL https://doi.org/10.1007/s11071-012-0507-y
31. Maachou, A., Malti, R., Melchior, P., Battaglia, J.L., Oustaloup, A., Hay, B.: Nonlinear thermal system identification using fractional volterra series. Control Engineering Practice **29**, 50 – 60 (2014)
32. Malti, R., Sabatier, J., Akçay, H.: Thermal modeling and identification of an aluminum rod using fractional calculus. IFAC Proceedings Volumes **42**(10), 958 – 963 (2009). DOI https://doi.org/10.3182/20090706-3-FR-2004.00159. 15th IFAC Symposium on System Identification
33. Mani, A.K., Narayanan, M.D., Sen, M.: Parametric identification of fractional-order nonlinear systems. Nonlinear Dynamics (2018). DOI 10.1007/s11071-018-4238-6. URL https://doi.org/10.1007/s11071-018-4238-6
34. Monje, C.A., Chen, Y., Vinagre, B.M., Xue, D., Feliu-Batlle, V.: Fractional-order systems and controls: fundamentals and applications. Springer Science & Business Media (2010)
35. Nise, N.: Control systems engineeringl, 6 edn. Wiley (2011)
36. Petras, I.: Fractional-order nonlinear systems: modeling, analysis and simulation. Springer Science & Business Media (2011)
37. Raja, M., Chaudhary, N.: Adaptive strategies for parameter estimation of box-jenkins systems. IET Signal Processing **8**, 968–980(12) (2014)
38. Sheng, H., Chen, Y., Qiu, T.: Fractional processes and fractional-order signal processing: techniques and applications. Springer-Verlag London Springer (2012)
39. Sierociuk, D., Dzielinski, A.: Fractional kalman filter algorithm for the states, parameters and order of fractional system estimation. International Journal of Applied Mathematics and Computer Science **16**(1), 129 (2006)
40. Simpkins, A.: System identification: Theory for the user, 2nd edition (ljung, l.; 1999) [on the shelf]. IEEE Robotics Automation Magazine **19**(2), 95–96 (2012). DOI 10.1109/MRA.2012.2192817
41. Soltan, A., Radwan, A., Soliman, A.M.: Butterworth passive filter in the fractional-order. In: International Conference on Microelectronics, pp. 1–5. IEEE (2011)
42. Soltan, A., Radwan, A., Soliman, A.M.: Fractional order filter with two fractional elements of dependant orders. Microelectronics Journal **43**(11), 818–827 (2012)
43. Tang, Y., Zhang, X., Hua, C., Li, L., Yang, Y.: Parameter identification of commensurate fractional-order chaotic system via differential evolution. Physics Letters A **376**(4), 457 – 464 (2012)
44. Tepljakov, A., Petlenkov, E., Belikov, J.: Fomcon: Fractional-order modeling and control toolbox for matlab. In: Proceedings of the 18th International Conference Mixed Design of Integrated Circuits and Systems - MIXDES 2011, pp. 684–689 (2011)
45. Tsang, K., Billings, S.: Identification of continuous time nonlinear systems using delayed state variable filters. International Journal of Control **60**(2), 159–180 (1994)
46. Verhulst, F.: Nonlinear differential equations and dynamical systems. Springer Science & Business Media (2006)
47. Victor, S., Malti, R., Garnier, H., Oustaloup, A.: Parameter and differentiation order estimation in fractional models. Automatica **49**(4), 926 – 935 (2013). DOI http://dx.doi.org/10.1016/j.automatica.2013.01.026
48. Wang, L., Gawthrop, P.: On the estimation of continuous time transfer functions. International Journal of Control **74**(9), 889–904 (2001). DOI 10.1080/00207170110037894
49. Welty, J.R., Wicks, C.E., Rorrer, G., Wilson, R.E.: Fundamentals of momentum, heat, and mass transfer. John Wiley & Sons (2009)
50. Wiener, D., SPINA, J.: Sinusoidal Analysis and Modelling of weakly Non-linear Circuits. New York: Van Nostrand Reinhold (1980)
51. Winder, S.: Analog and digital filter design. Newnes (2002)
52. Young, P.C.: Recursive estimation and time-series analysis: An introduction for the student and practitioner. Springer Science & Business Media (2011)
53. Zhang, B., Billings, S.: Identification of continuous-time nonlinear systems: The nonlinear difference equation with moving average noise (ndema) framework. Mechanical Systems and Signal Processing **60**, 810 – 835 (2015)
54. Zhao, Y., Baleanu, D., Cattani, C., Cheng, D., Yang, X.: Maxwell's equations on cantor sets: a local fractional approach. Advances in High Energy Physics **2013** (2013)